RESERVOIR STEAM FLOOD MODELING BASED ON 4D SEISMIC AND ROCK PHYSICS

Muhammad Edisar
Usman Malik
Computational of Phyfsics and Earth Science Laboratory Physic Dept. Riau University
Email : edisar_m@yahoo.com

ABSTRACT

Reservoir steam flood modeling based on Time Lapse (*4D*) seismic and Rock Physics data was constructed in Pelangi oil field on central Sumatra Basin. Model used to monitoring and tracking steam flood and production related changes in the reservoir. A model of the reservoir steam flood was constructed for a pattern steam flood in Area X of the field. The model was based on a geostatistical geological model and populated with temperature and porosity. Pressure and saturation properties were added to provide the necessary input for seismic modeling. Through a rock physics model based on the core analysis, the elastic properties (Vp, Vs and density) were determined. These elastic properties were used to determine the seismic response of the model with and without steam flood.

The results of the model indicated, that from the rock physics modeling using Gassmann equation, steam flood decreases the V_p by an average of 20-25% in the reservoir sands. Rock physics analysis also shown that shear velocities are also sensitive to steam flood, with an average decrease of 12%. However, the Gassmann calculation results shown that V_s is insensitive to steam flood. This discrepancy is probably caused by Gassmann's assumptions that no chemico-physical interactions exist between the rocks and pore fluids. Time shifts in seismic modeling events provided an indication of the presence of steam flood in the overlying reservoir. The relationship between time shift and steam thickness was strong for thick steam, but it was not possible to distinguish thin steam zones from thick hot oil zones solely on the basis of time shift. At the same time, tuning between the steams related and geologically related seismic events influenced seismic amplitudes. It appears that a combination of attributes is necessary to resolve the effects of steam on the 4D seismic data acquired over of the field.

Keywoods : *Reservoir, Seismic, Rock*

INTRODUCTION

During the last two decades, a number of successful strategies have emerged for detecting hydrocarbons from seismic data. Most of these are based on rock elastic properties, travel time (*or velocity*), impedance, bright spots and can be understood

deterministically in terms of the compressibility and density of the pore fluids, coupled with the stiffness of the rock matrix. The mechanics of these elastic fluid signatures at low seismic frequencies are described by the well-known *Gassmann (1951)* relations. AVO analysis, which uses inference of both P and S-wave impedances helps to separate pore fluid from lithologic effects (*Ostrander, 1984; Smith and Gidlow, 1987*). However, many problems remain, especially the detection of low gas saturation, oil water contact (*OWC*), gas oil contact (*GOC*) and seismic attenuation still difficult to resolve from seismic, using rock physic and seismic modeling and correlated to seismic and well log data will provides an additional discriminator for hydrocarbon indicator (*Edisar at al., 2004*).

Hydrocarbon production directly affects the reservoir properties (*saturation gas, oil and water, pressure and temperature*). In order for time-lapse (*4D*) monitoring to be effective, the changes in reservoir properties must cause a detectable change in the seismic parameters (*Edisar, 2000*). In this case rock physics relationships provide the bridge between the primary reservoir properties and the seismic parameters. 4D seismic technology is a volume resolution enhancing used to monitoring of reservoir parameters properties changes respect to lapse time. Petrophysic data

and seismic are important information for static and dynamic reservoir characterization such as porosity, saturation and fluid distribution properties (*Edisar, 2002*). One of the most common rock physics modeling processes is based on the theories of Biot and Gassmann for determining the properties of fluid saturated rock from the properties of dry or air filled rock. Particular care is taken to use realistic solid mineral properties in the Biot-Gassman transform. For example calibrate the clay bulk modulus and density and then compute the correct average solid moduli and density at each depth sample. This gives more accurate results than the common block or zone averaging approach. Fluid properties are also carefully computed using either homogenous or "patchy" fluid mixing rules to give the correct results. This avoids the problem of over or under predicting fluid saturation effects that can occur with more simplistic approaches (*Edisar et al., 2004*).

In this study, we attempted to understand the seismic and rock physic of reservoir response with respect to steam flood from a forward modeling approach. In this methodology, a model is constructed and the resultant seismic cube interpreted in a similar manner to the real seismic data on the field. Since the properties of the model are known, we can obtain insights into the usefulness and

pitfalls of different interpretation methodologies. Comparing properties predicted from the synthetic seismic data to the properties used to construct the synthetic seismic data could do this. The process of synthetic seismic modeling involves the following steps: (1) Rock physics modeling (2) Construction of static (facies and porosity) and dynamic reservoir (temperature, pressure and saturation) property earth model. (3) Calculation of the elastic properties (*Vp, Vs and density*) from the dynamic and static reservoir properties using an appropriate rock physic model. (4) Calculation of reflectivity and convolution with an appropriate seismic wavelet to output a synthetic seismic model.

Interpretation of the model involved rock physics analysis result, analysis of the amplitudes, time shifts and reservoir properties versus the seismic parameter caused by the presence of the steam. Despite of the limitations, the model provides some idea of the usefulness and potential pitfalls of relying on each of the interpretation techniques.

FLUID SUBTITUTION MODELING

Fluid properties can be estimated using relationships (*Batzle and Wang, 1992*). These relationships are based on empirical measurements. Fluid calculating requires oil API gravity, gas gravity, *GOR*, reservoir pressure, and temperature. Brine salinity is also required. In case of Pelangi field the pore fluid/reservoir pressure varied from 50 psi to 350 psi. The *API* gravity is around 20^om and salinity assumed 5000 ppm for the water. The elastic properties (*modulus and velocity*) of the reservoir oil and water were then calculated. At 350° F, water will become steam when pressure is below 135 psi. As a result, for simply assumed a bulk modulus of 0.2 GPa and a bulk density of 0.2 g/cm^3 for steam. Velocities in oil/water-saturated rocks were calculated using the Gassmann equation (*Gassmann, 1951*):

$$K_{sat} = K_{dry} + \frac{(1 - K_{dry}/K_m)^2}{\dfrac{\phi}{K_f} + \dfrac{1-\phi}{K_m} - \dfrac{K_{dry}}{K_m^2}}, \qquad (1)$$

Where K_{sat} is the bulk modulus of a rock saturated with a fluid of bulk modulus K_f, K_d is the frame (*dry*) bulk modulus, and K_m is the matrix (*grain*) bulk modulus of the same rock, and ϕ is the porosity. The shear modulus G_{sat} of the rock is not affected by fluid saturation, so that

$$G_{sat} = G_{dry}, \qquad (2)$$

Where G_{dry} is the frame (*dry*) shear modulus of the rock. The density ρ_{sat} of the saturated rock is simply given by

$$\rho_{sat} = \rho_{dry} + \phi\rho_f. \qquad (3)$$

Where ρ_{sat} and ρ_{dry} are the fluid-saturated and dry densities of the rock, respectively. ρ_f is the pore fluid's density. The frame bulk and shear moduli were calculated using the measured velocities in the frame rock:

$$K_{dry} = \rho_{dry}\left(V_p^2 - \frac{4}{3}V_s^2\right), \qquad (4)$$

$$G_{dry} = \rho_{dry}V_s^2. \qquad (5)$$

The bulk modulus K_f of the oil/water mixture was calculated using Wood's equation (*Wood, 1930*)

$$\frac{1}{K_f} = \frac{1-S_o}{K_w} + \frac{S_o}{K_o}, \qquad (6)$$

Where K_w and K_o are the bulk moduli of water and oil, respectively, and S_o is the oil saturation in fraction. The bulk density ρ_f of the oil/water mixture is calculated by

$$\rho_f = (1-S_o)\rho_w + S_o\rho_o \qquad (7)$$

Where ρ_w and ρ_o are the bulk densities of water and oil, respectively.

In the Gassmann calculation, assumed that the pore spaces were occupied by only water and oil no gas is present and also assumed a grain (*matrix*) bulk modulus, K_m, of 38 GPa for the sands and shales and 76 GPa for other samples with high grain densities. For each sample selected for temperature measurements from 75° to 350° F, on the velocities, which is defined as (*Wang, 2001*)

$$\Delta V(\%) = \frac{Vat350^o\,F - Vat75^o\,F}{Vat75^o\,F}x100\% \quad (8)$$

Where V can be either compressional (V_p) or shear (V_s) velocity.

At 350° F, water in the pore space will transform to steam whenever the reservoir pore fluid pressure drops below 135 psi. Therefore, the measured velocity changes at 100 and 50 psi are caused by both the temperature increase and the presence of steam. Since define the effect of steam injection at these reservoir pressures on the measured and calculated seismic properties as, here V_p as an example (*Wang, 2001*).

$$\Delta V_p = \frac{V_{p350^o\,F} - V_{p75^o\,F}}{V_{p75^o\,F}} \times 100\%, \qquad (9)$$

Where $V_{p350^o\,F}$ and $V_{p75^o\,F}$ are the measured compressional velocities at 350° F and 75° F, respectively.

The changes in seismic properties in the above discussion are caused by the combined effect of increase in temperature and presence of steam in the rock. For each sample, also tried to separate the effect of temperature from that of steam. Assuming that there was no free steam in the pore space so

that the effect of temperature alone can be defined as (V_p as an example)

$$\Delta V_p = \frac{ExtrpV_{p350^o F} - MeasV_{p75^o F}}{MeasV_{p75^o F}} x100\% \quad (10).$$

The effect of steam aloneis therefore defined as

$$\Delta V_p = \frac{MeasV_{p350^o F} - ExtrpV_{p350^o F}}{ExtrpV_{p350^o F}} x100\% \quad (11)$$

The effect of steam alone was calculated using the extrapolated seismic properties, assuming no phase changes in the pore fluids, at 100-psi reservoir pore pressure and 350° F. By comparing the extrapolated data with the measured data, one is able to quantify the effect of steam in the pore space on the seismic properties. The changes in seismic properties due to the presence of steam can be correlated to porosity. For the velocity changes (*Wang, 2001*),

$$\Delta V_p \approx -0.153\phi - 2.118 \quad (12)$$

$$\Delta V_s \approx 0.11\phi + 0.5 \quad (13)$$

Where ΔV_p and ΔV_s are the percentage changes in compressional and shear velocities,ϕ=Porosity

P and S wave velocities increase with pressure.Increasing pressure closes cracks and pores in the rock frame. Two types of pressure affect seismic velocities; Overburden pressure: Combined weight of rock and fluids above reservoir (*Mavko et al, 1998*).

$$S = g\sum_{0}^{z} \rho_b(z)dz \quad (14)$$

Normal gradient is 1.0 psi/ft or 0.0225 MPa/m

Hydrostatic (*pore or reservoir*) pressure weight of the fluid column

$$P_H = \rho_{fl}gz \quad (15)$$

Normal gradient is 0.465 psi/ft or 0.0105 MPa/m. Where g is gravity, ρ_b and ρ_{fl} are bulk and fluid density respectively and z is depth. Seismic velocity is primarily influenced by effective pressure:

$$P_{eff} = S - P_H \quad (16)$$

The rock physics and seismic modeling relationships are based on real core data measured on frame rocks that allows one to model seismic responses to fluid saturation and pressure changes. The frame bulk and shear moduli were calculated using the measured velocities and bulk densities. Statistical relationships between the frame bulk and shear moduli and porosity were obtained through linear correlations (*Wang, 2001*)

$$K_{dry} = a + b\phi \quad (17)$$

And

$$G_{dry} = c + d\phi \quad (18)$$

Where porosity ϕ is in fraction, K_{dry} and $G_{dry}$are in **GPa** (*Gigapascal*).

In order to obtain meaningful statistical relationships, normally measured a large number of samples from each reservoir/field to minimize the effect of heterogeneity and scaling. The coefficients *a, b, c*, and *d* in equations (17) and (18) are obviously dependent on the net overburden pressure. It is the net overburden pressure (*also called differential pressure or sometimes effective pressure*) that governs the elastic properties of reservoir rocks. Therefore further we can correlate the coefficients *a, b, c*, and *d* to the net overburden (*effective*) pressure P_{eff}

$$a = a_o + a_1 P_{eff} + a_2 \sqrt{P_{eff}} \qquad (19)$$

$$b = b_o + b_1 P_{eff} + b_2 \sqrt{P_{eff}} \qquad (20)$$

$$c = c_o + c_1 P_{eff} + c_2 \sqrt{P_{eff}} \qquad (21)$$

$$d = d_o + d_1 P_{eff} + d_2 \sqrt{P_{eff}} \qquad (22)$$

all the measured Pelangi sands. The correlation coefficients result are listed in the (*Table.1*).

MODEL BUILDING

The input object for the seismic modeling tools are the Sgrid in depth, porosity, water saturation, oil saturation, gas saturation, P-wave velocity, density, facies, pore pressure, temperature, solvent saturation and S-wave velocity. In this case we looked at for Duri Technical Team, PT. CPI, built a style of simulation model. The porosity, permeability and temperature were geostatistically simulated across the Area-X 7-spot steam pattern of Pelangi field central Sumatra basin (*Figure 1a*). Vertical cell thickness averaged 0.8 feet (*0.25m*). It was necessary to add
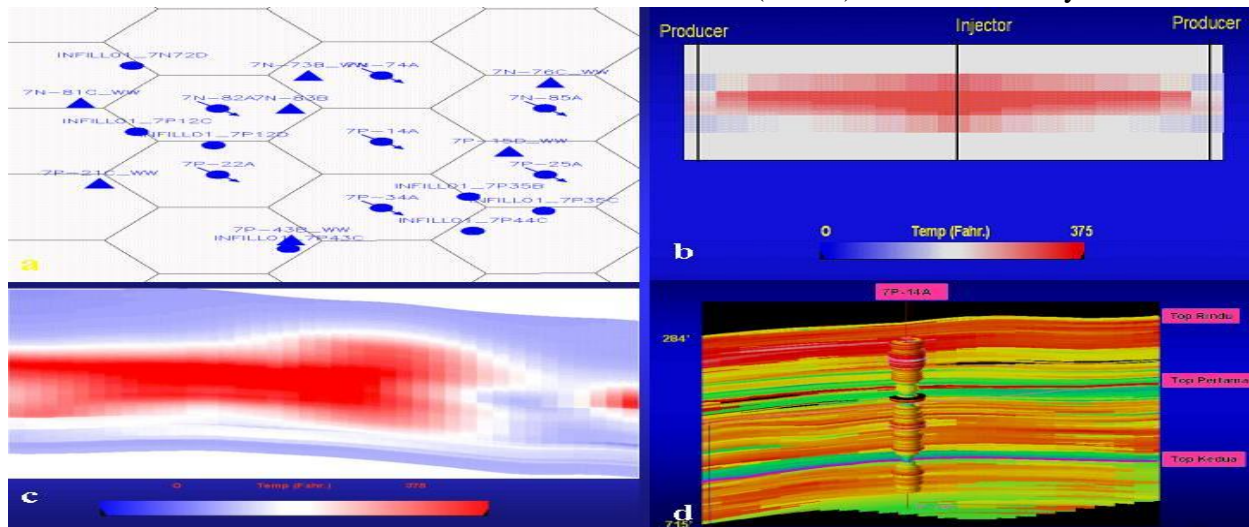
(Figure 1.a)

Where the net overburden (*effective*) pressure. P_{eff} is in psi. For the correlations on

pressure and saturation properties, and to modify the temperature property. Pressure was

determined from consideration of the likely bottomhole pressure in the injectors and producers (*Figure 1b*). Temperature was reset to a constant gradient where the temperature was less than 320F (160C). It was necessary to ensure that temperature and pressure conditions were appropriate for steam generation. Saturations was assigned on the following basis:

Initial Conditions

Water: $Sw_0 = 1.45 \log \{Permeability\}-0.37$

Oil: $So_0 = 1-Sw$

Gas: $Sg_0 = 0.0$

Steam: $Ss_0 = 0.0$

Temp: $Tm_0 = 90+0.262.\text{Depth}$ (*TVDSS*)

Steamed Conditions

$Sw_1 = Sw_0 \times 0.9$ for Temp change > 210F

$So_1 = So_0 \times 0.117$ for Temp Change > 210F

$Sg_1 = 0.0$

$Ss_1 = 1-Sw-So-Sg$

Temp: Reset to $90+0.262.\text{Depth}$ (*TVDSS*)

Where Tm < 160CBecause temperature was built using the TO wells, and not including the injection wells, the greatest steam thickness is located over the TO wells, and not the injectors. The temperature logs also show a broad decline above and below hot zones, and it was necessary to remove this for the model to adequately generate a seismic response to steam. Review of the model after

analysis showed that there was more steam in the model than was likely in the real subsurface. The wireline logs show that the amount of steam in the section occurs in much more limited intervals than the temperature profile. The temperature logs taken on their own therefore appear to over-estimate the amount of steam in the subsurface. Despite this, the decision was taken to use this model since it provided an appropriate variety of geological and steam conditions.

ELASTIC PROPERTIES CALCULATION

The function of this step is to transform the reservoir properties (*porosity, facies, saturation ect*) into elastic properties (*Vp, Vs, Density*). Using the Batzle-Wang relationships (*Batzle and Wang, 1992),* the elastic properties *Vp, Vs* and *Density* were determined for the sands of the reservoir using a rock physics model built from the core analysis carried on Pelangi field samples (*Edisar at al., 2004*). The fluid properties necessary for these equations were: Gas-oil Ratio: 0, Oil Gravity: 20 degrees API, Water Salinity: 5000 ppm. The dry frame bulk (*K*) and shear (*G*) moduli were determined from the following relationships (*Wang, 2001*)

$$K_{dry} = a_o + a_1 P_{eff} + a_2 \sqrt{P_{eff}} +$$

$$\phi\left(b_o + b_1 P_{eff} + b_2 \sqrt{P_{eff}}\right) \qquad (23)$$

$$K_{dry} = c_o + c_1 P_{eff} + c_2 \sqrt{P_{eff}} +$$

$$\phi\left(d_o + d_1 P_{eff} + d_2 \sqrt{P_{eff}}\right) (24)$$

$$\rho_{dry}\left(g/cm^3\right) = \rho_{grain}\left(1-\phi\right) \qquad (25)$$

Where the scalar in this equation are derived from core analysis (*Table. 1*).

P_{eff} =(*Lithostatic Pressure – Pore Pressure) in psi*, ρ_{grain} = 2.64 *g/cm³ and* ϕ = *Porosity.*

While the dry frame and fluid properties were combined to generate the fluid-saturated bulk and shear moduli, and density, using the Gassmann equation in equation (*1*), (*4*), (*5*) and (*7*) the above.

SEISMIC MODELING

The seismic modeling step inputs the *Vp, Vs* and *Density* properties, converts from time to depth, determines reflectivity with offset and outputs the convolved seismic trace. At each XY location, PP and PS reflection mode are derived from *Aki-Richards (1980)*

$$R_{pp} = \left(1 - 4p^2 V_s^2\right)\frac{\Delta\rho}{\rho} + \left(\frac{1}{2}\cos^2\theta\right)\frac{\Delta V_p}{V_p} - \left(4p^2 V_s^2\right)\frac{\Delta V_s}{V_s} \quad (26)$$

$$R_{ps} = \left(\frac{pV_p}{2\cos\varphi}\right)\left\{\left(4V_s^2 p^2 - \frac{4V_s^2\cos\theta\cos\varphi}{(V_p V_s)}\right)\frac{\Delta V_s}{V_s} - \right.$$

$$\left.\left(\frac{1 - 2V_s^2 p^2 + 2V_s^2\cos\theta\cos\varphi}{(V_p V_s)}\right)\frac{\Delta\rho}{\rho}\right\} (27)$$

$$R_{ss}(\theta) = \frac{1}{2}\left(\frac{1}{2}\cos^2\theta - 4p^2 V_s^2\right)\frac{\Delta V_s}{V_s} + \frac{1}{2}\left(1 - V_s^2 p^2\right)\frac{\Delta\rho}{\rho}$$

$$(28)$$

Where:

$$p = \frac{V_p}{\sin\theta}; \qquad \cos\varphi = 1 - \left(\frac{V_s}{V_p}\right)\sin^2\theta$$

Seismic reflection models deal with the interface between the top (or base) and what is above it (or below it). To determine the acoustic impedance change at the interface for normal incidence set $\theta = 0$, then the equation can be written as:

$$I_P = \frac{\left(V_{p(n+1)}\rho_{(n+1)}\right) - \left(V_{p(n)}\rho_{(n)}\right)}{\left(V_{p(n+1)}\rho_{(n+1)}\right) + \left(V_{p(n)}\rho_{(n)}\right)} \qquad (29)$$

Where n = *1, 2, 3,... N* (*number of layer*)

To build of seismic modeling, specify the source-receiver offset ranges that we wish model. These offsets will be converted to incident angles for the reflectivity calculation. Noffset is the number of offsets, Offset0 is the first offset, and Δoffset is the increment. Note that:

$$MaxOffset = (Noffset - 1)\Delta Offset \qquad (30)$$

Reflectivity was determined for the 8 offsets in the range 0-975 feet (*0-297m*). Each offset was convolved with zero phase Butterworth filter of 10-70 Hz frequency with 36dB/octave roll off at either end. The offset traces were stacked to produce a single trace at each location.

490

ROCK PHYSIC MODELING

Calculated P-wave and S-wave impedances are using the bulk density and compressional and shear velocities. The velocities and bulk density were calculated using the Gassmann equation and the measured dry frame rock properties under reservoir saturation, pressure, and temperature conditions. All the samples were saturated with oil at $S_{steamirr}$. For laboratory steam flood experiments, the samples were re-saturated with reservoir-equivalent hydrocarbon oil at irreducible steam saturations. Steam flood was performed and seismic properties were monitored. The measured magnitude of V_p changes as the oil saturated (*at irreducible steam saturation*) samples are flooded with steam at a constant net overburden pressure of 350 psi (*Figure 2a,b,*).

The results indicated that from the rock physics modeling using Gassmann equation, steam injection decreases the V_p by an average of 20-25% in the reservoir sands. The analysis also shows that shear velocities are also sensitive to steam injection, with an average decrease of 12%. However, the Gassmann calculation results show that V_s is insensitive to steam injection. This discrepancy is probably caused by Gassmann's assumptions that no chemico-physical interactions exist between the rocks and pore fluids. Velocity changes as a function of pressure and temperature. Velocity decreases during the primary production cycle before steam injection due to the presence of evolved hydrocarbon gas (*point 1 to 2 figure 2c*). At the beginning of steam injection the free gas is pushed back into solution and there is a
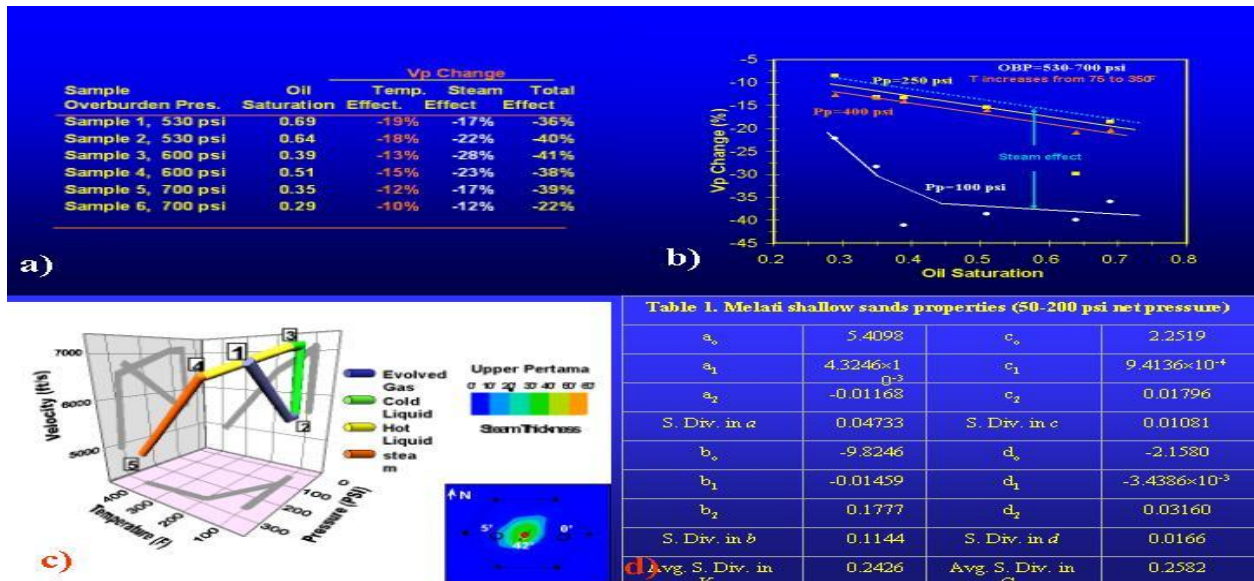
(*Figure 2a,b,*).

velocity increase (*point 2 to 3 figure 2c*). As steam injection continues, a velocitydecrease is due to heat (*point 3 to 4 figure 2c*) and finally due to steam (*point 4 to 5 figure 2c*). From the rock physics modeling and analysis resulted sand properties parameters (*Table 1 figure 2d*). These parameters will be used for synthetic seismic modeling.

SEISMIC SYNTHETIC SEISMIC MODEL

The seismic response to steam flooding is manifested in two key attributes amplitude and time shift. There are other potential attributes Vp/Vs ratio from the amplitude gradient of the prestack gathers, and measures of attenuation through the low impedance steam zones, but these were not investigated in this modeling workflow, but represent possible avenues to explore in the future. The time section summarizes the results of the synthetic seismic model (*Figure 3a*). There are a number of events on the pre-steam model that are generated by the static geological model. The steamed model shows two additional seismic reflections from the top and base of the steam zone. At the top of the steam there is an increase in amplitude where the top steam event constructively interferes with the Top Pertama seismic event. At the base of steam there is destructive interference between the

base steam and Top Kedua seismic event. The implication is that amplitude is potentially affected by interference between the steam and the geological seismic markers. While this potentially complicates the interpretation of the seismic amplitudes, it also potentially provides information as to the location of the steam within the section, and the proximity of the steam to the Top Pertama and Kedua. To compare the synthetic seismic modeling section correlated to the monitor real seismic section (*Figure 3b*) and also we can see that steam monitoring are different using seismic and without seismic. The temperature well shows steam in Upper Pertama has highest permeability, also the data indicates high injection into both Upper and Lower Pertama, low injection into Kedua (*Figure 3c and Figure 3d*).

The time shift is caused by the change in interval transit time of the reservoir, and results from the decrease in P-wave velocity due to steam. The expected response can be calculated from the input model using the pre-steamed and steamed P-wave velocity property. For each XY location:

$$Timeshift = \frac{\sum DZ}{\left(V_{p(unsteamed)} - \frac{Z}{V_{p(steamed)}}\right)} \quad (12)$$

DZ = *Vertical cell thickness*

Time shift is positive downwards. Equation (12) can be used to compare the fidelity of the time shift methodologies.

The time shift information can be determined by two methods: subtraction of time structure of an event on both seismic cubes, or determination of the time shift necessary to maximize the correlation coefficient between the two cubes, in an appropriate time window. Note that the time shift is determined by the velocities overlying the reference horizon or correlation time window.

SEISMIC TIME SHIFTS OF THEMODEL

The cross plots the time shift against the known steam thickness was built (*Figure 5d*). At large steam thickness there is a strong
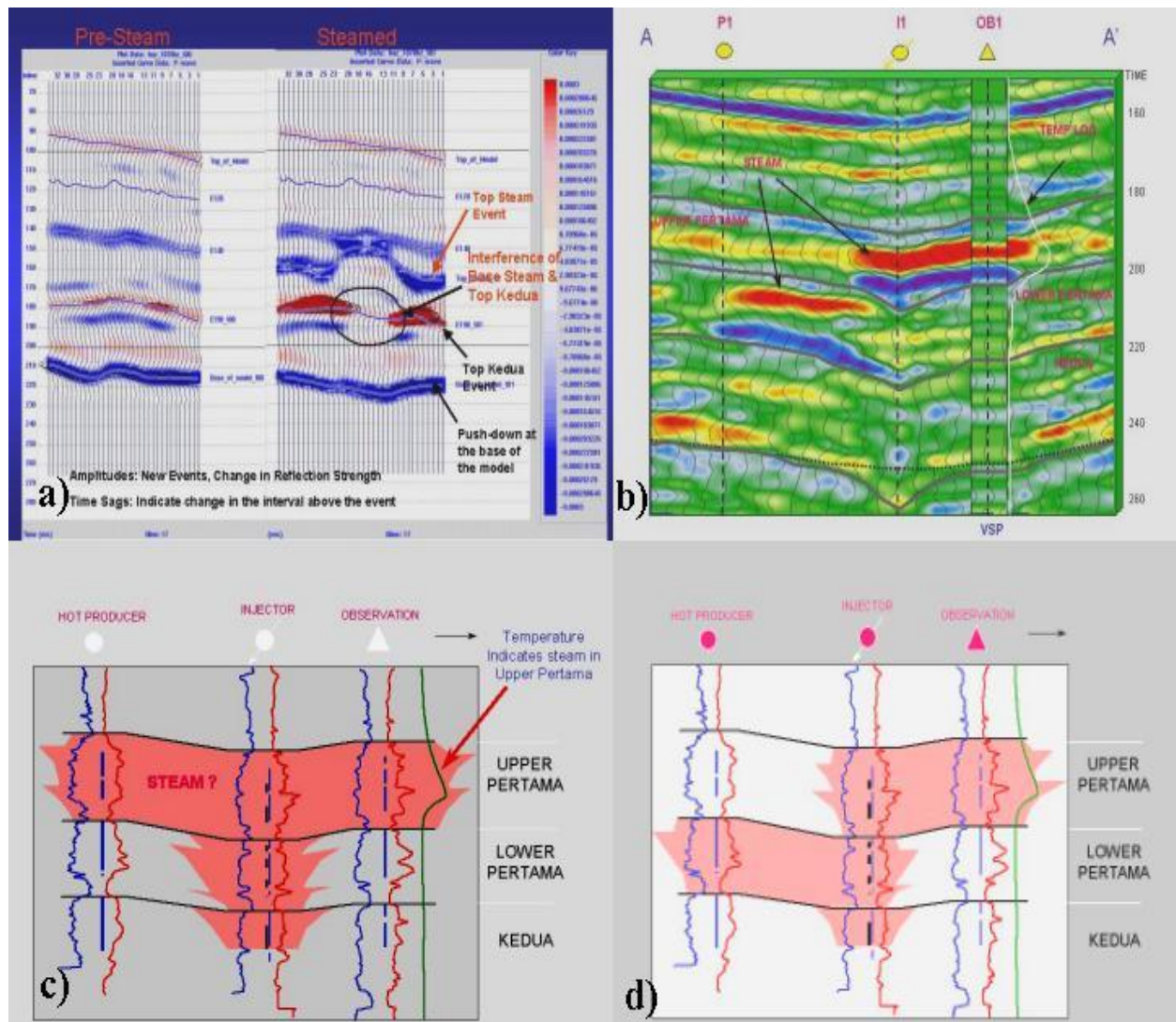
(*Figure 5a,b,c,d*).   there is more scatter.

We speculate that this is due to additional time shifts from hot oil zones, or to the presence of hot water, rather than steam in the reservoir. Both of these conditions would produce a similar magnitude of time shift. (*Figure 4A*) shows the distribution of calculated tTime shift from the change in P-wave velocity between the pre-steamed and steamed synthetic model cases. (*Figure 4B*) shows the time shift calculated at the base of the model using cross-correlation of trace methods. The maximum time shift is 16mS, corresponding to a cumulative steam thickness of 220 feet (67m). Some errors occur due to errors in the horizon interpretation, and so the method is dependent upon the amplitude and the continuity of the reference seismic horizon.

Determining the time shift necessary to maximize the correlation coefficient between traces is also reliable under these conditions (*Figure 4C and 5C*).

SEISMIC TIME SHIFTS MODEL AT THE TOP KEDUA FORMATION

The process repeated for the Top Kedua formation, and the calculated time shifts are shown in (*Figure 4d*). The time shifts calculated from the horizon interpretation show that this method is under-estimating the amount of time shift on this horizon. This is because of the interference between the base steam event and the Top kedua formation event. In the interference zone, the peaks and troughs no longer correspond with either the geological or steam event. Under this condition, using the cross-correlation method works better (*Figure 4c*), because the result is based on wider time window and so is driven more by the lower amplitude events above and below the Kedua, where there is less interference.

AMPLITUDE ANALYSIS AT TOP PERTAMA

If we looked at the amplitudes at the Top pertama event in the model (*Figure 5b*). Here we can see where expected to see high amplitudes associated with the steam, we see low amplitudes. Again, this relates to the interference between, in this case, the Top steam and the Top pertama events. Away from the area of interference, the amplitudes are reasonably consistent with the presence of steam and the unsteamed zone on the east of the model can be identified.

CONCLUSION

The Rock physic analysis and synthetic seismic modeling provides us with insights into the relationship between seismic and reservoir properties. It is not necessarily (*though ideally it should be*) to have an accurate model of the subsurface, but captures the variability of the important parameters in the subsurface. The use of geostatistical properties tends to over estimate the amount of steam in the section, so the model is biased towards a thick steam zone.

For interpretation, we can conclude:

1) Seismic and Rock physic modeling have provided some insights into the detectability of steam and the usefulness of seismic attributes in determining the presence of steam.

2) Time shifts should play a role in the interpretation of the steam flood response, but the attribute is poor at distinguishing thick hot oil zones from thin steam zones. It is at best an indicator of heat.

3) Horizon-based methods for determining time shift should work for strong events below the steamed zone, where there is not interference between steam and geological seismic events.

4) Cross-correlation methods will work better for horizons closer to the steam zone, where there is a possibility of interference between steam and geological seismic events.

5) Amplitudes may be a useful indicator of steam, except where the steam is thick enough to cause interference with high amplitude geologically related seismic events. Recognition of where this occurring may be important for the calibration of seismic amplitude to steam.

ACKNOWLEDGEMENTS

REFERENCES

Aki, K.,and Richards, P.G., 1980, *Quantitative seismology; Theory and methods*; W.H. Freeman and Co.

Batzle, M.,and Wang, Z., 1992, *Seismic properties of pore fluids:* Geo-physics,**5**7, 1396–1408.

Edisar. M, Handayani.G, Subiyanto. B, 2000, *Proses dan analisis data seismik 3D dan 4D untuk monitoring injeksi steam lapangan*

"Losf 588" PT. Caltex Pacific Indonesia, Tesis, Geofisika Terapan, ITB Bandung.

Edisar. M, 2002, *Optimasi cross-equalisasi seismik time-lapse (4-D) untuk monitoring dan karakterisasi sifat dinamika reservoir lapangan "mory",* Proceeding, The HAGI 27th annual meeting-Malang.

Edisar.M, Hendrajaya.L., Handayani.G., Fauzi.U., Yarmanto., 2004, *Seismic and rock physics diagnostic to predict porosity and fluids saturation,* Proceeding, The HAGI 29th annual meeting-Yogyakarta.

Edisar.M, Hendrajaya.L., Handayani.G., Fauzi.U., Yarmanto., 2004, *Predicting porosity and saturation from acoustic velocities based on rock physics diagnostic*, Proceeding, Simposium Nasional & Kongress VIII, IATMI, (*29 Nov-01 Desember*), Jakarta

Gassmann, F.,1951, *Elastic waves through a packing of spheres:* Geophysics, **16**, 673-685

Mavko, G., Mukerji, T., and Dvorkin, J., 1998, *The rock physics handbook: Tools for seismic analysis in porous media*: Cambridge Univ. Press.

Ostrander, W., J., 1984, *Plane-wave reflection coefficients for gas sands at non-normal incidence:* Geophysics, Vol. 49, p1637-1648.

Smith, G.C., and Gidlow, P.M., 1987, *Weighted stacking for rock property estimation and detection of gas*; Geophys. Prosp., 35, 993-1014.

Widyantoro,A.,Primadi,H.,1998.*Understanding Steam Behavior of Area 5 Duri After Six years Injection,"* presented at the CPI Technology Meeting.

Wang.Z .,2001, Y2K, *Tutorial, Fundamentals of seismic rock physics,* Geophysics, vol. 66, no. 2 (March-April 2001); p. 398–412.

Wood, A. B., 1930, *A textbook of sound*: G. Bell and Sons, London

Figure 1. a) The simulation model, the porosity, permeability and temperature were geostatistically simulated 7-spot steam pattern **b)**Simulation model for steam rigorous fluid modeling average porosity by layer no
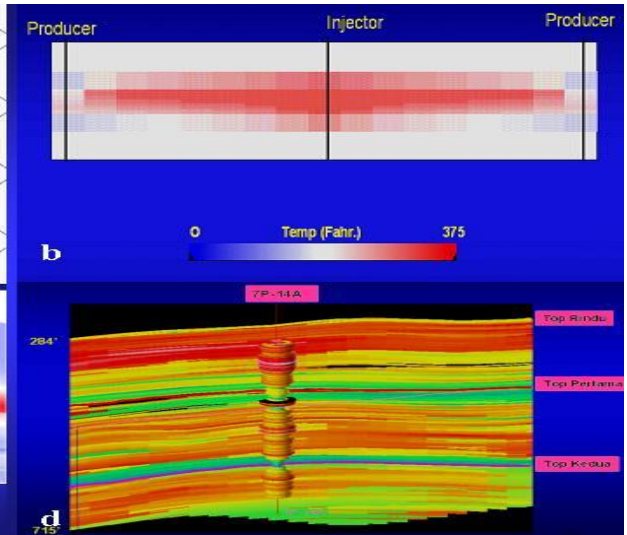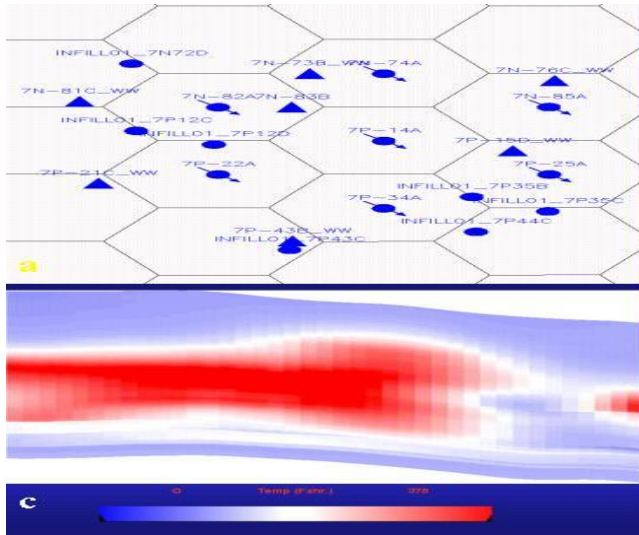
lateralheterogeneity spatially symmetrical**c)**Geological model for Steam, temperature simulated from logs greater variability in steam thickness multiple steam zones closer to complex reality **d)**Stratigraphic framework to synthetic seismic modelingchanges for a single cell in the model as a function of pressure and temperature. Changes in pore fluid are indicated with color. Velocity decreases during the primary production cycle before steam injection due to the presence of evolved hydrocarbon gas (*point 1 to 2*). At the beginning of steam injection the free gas is pushed back into solution and there is a velocity increase (*point 2 to 3*). As steam injection continues, a velocitydecrease is due to heat (*Point 3 to 4*) and finally due to steam (*point 4 to 5*). **d)** Parameter sand properties from rock physics analysis result used for seismic modeling.

Sample Overburden Pres.	Oil Saturation	Vp Change		
		Temp. Effect.	Steam Effect	Total Effect
Sample 1, 530 psi	0.69	-19%	-17%	-36%
Sample 2, 530 psi	0.64	-18%	-22%	-40%
Sample 3, 600 psi	0.39	-13%	-28%	-41%
Sample 4, 600 psi	0.51	-15%	-23%	-38%
Sample 5, 700 psi	0.35	-12%	-17%	-39%
Sample 6, 700 psi	0.29	-10%	-12%	-22%

Table 1. Melati shallow sands properties (50-200 psi net pressure)

a_o	5.4098	c_o	2.2519
a_1	4.3246×10^{-3}	c_1	9.4136×10^{-4}
a_2	-0.01168	c_2	0.01796
S. Div. in a	0.04733	S. Div. in c	0.01081
b_o	-9.8246	d_o	-2.1580
b_1	-0.01459	d_1	-3.4386×10^{-3}
b_2	0.1777	d_2	0.03160
S. Div. in b	0.1144	S. Div. in d	0.0166
Avg. S. Div. in K	0.2426	Avg. S. Div. in G	0.2582

Figure 2. a,b) Rock physics properties model showing the modeled response for the pre-steamed and steam reservoir cases, **c)**Velocity changes for a single cell in the model as a function of pressure and temperature. Changes in pore fluid are indicated with color. Velocity decreases during the primary production cycle before steam injection due to the presence of evolved hydrocarbon gas (*point 1 to 2*). At the beginning of steam injection the free gas is pushed back into solution and there is a velocity increase (*point 2 to 3*). As steam injection continues, a velocitydecrease is due to heat (*Point 3 to 4*) and finally due to steam (*point 4 to 5*). **d)** Parameter sand properties from rock physics analysis result used for seismic modeling.
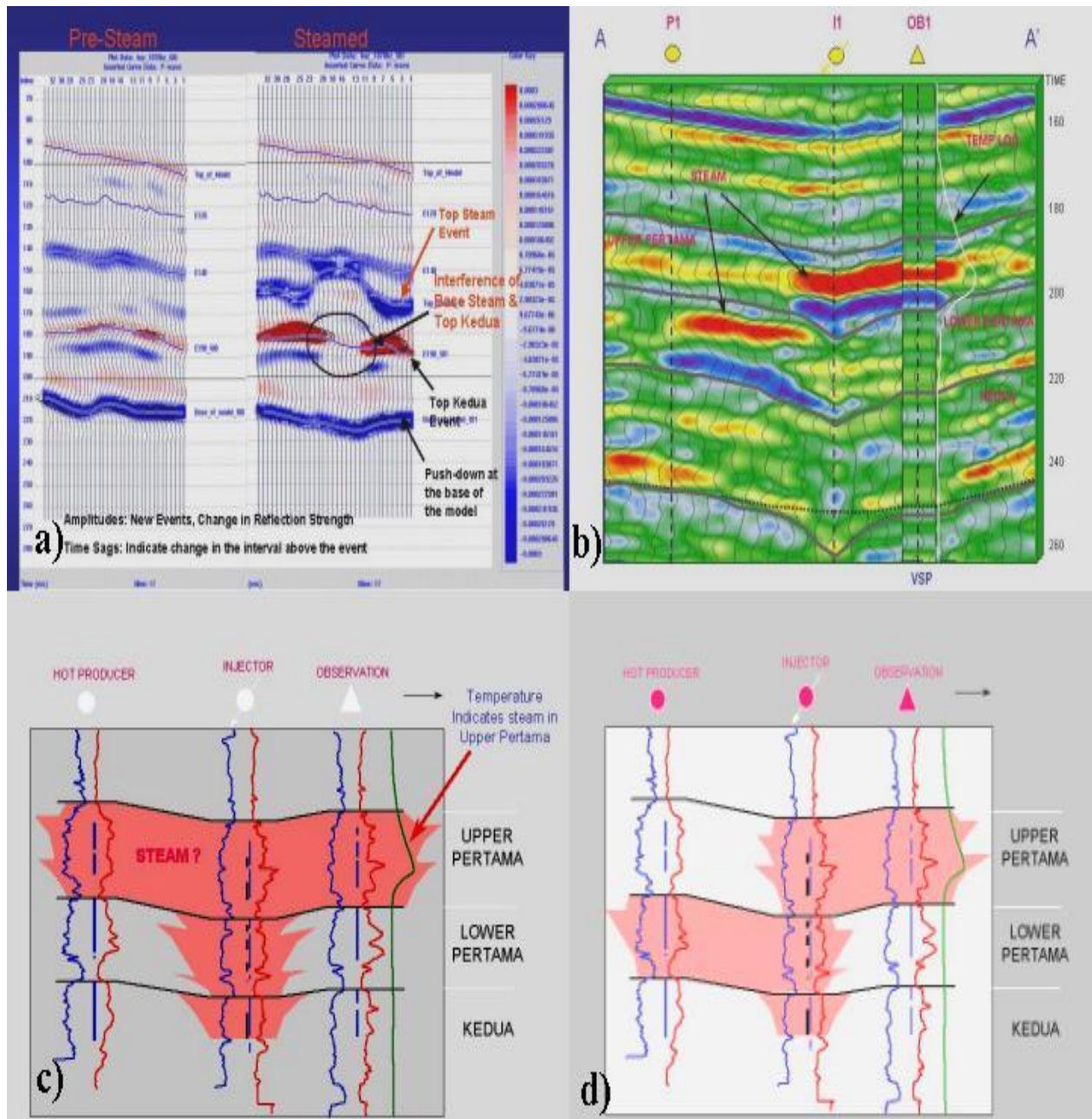
Figure 3. a) Seismic section through the synthetic seismic model showing the modeled response for the pre-steamed and steam reservoir cases, **b)** Monitor 1998 real Seismic section, **c)** Steam monitor without seismic, **d)** Steam monitor using seismic, temperature well shows steam in Upper PertamaUpper Pertama has highest permeability, data Indicates high injection into both Upper and Lower Pertama, low injection into Kedua

steamed and steamed synthetic model cases. **B)** The time shift calculated at the base of the model using cross-correlation of trace methods. **C)** Time Shift calculated at the Top Kedua from the change in P-wave velocity between the pre-steamed and steamed synthetic model cases. **D)**The time shift steam effect calculated from horizon time shift Top Kedua using interpretation of the pre-steamed
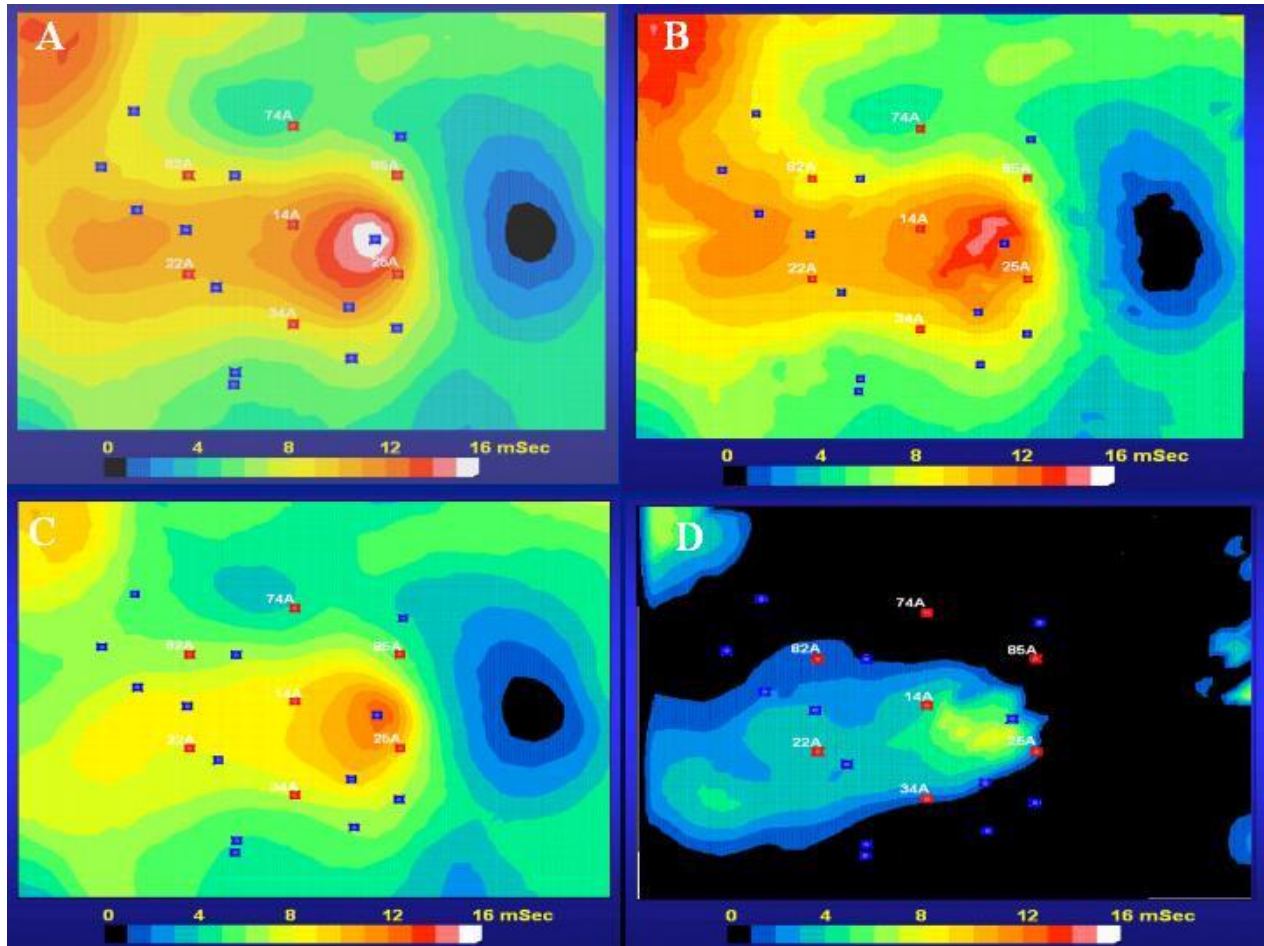
Figure 4.A) Time Shift calculated from the change in P-wave velocity between the pre-
and steamed synthetic seismic models.
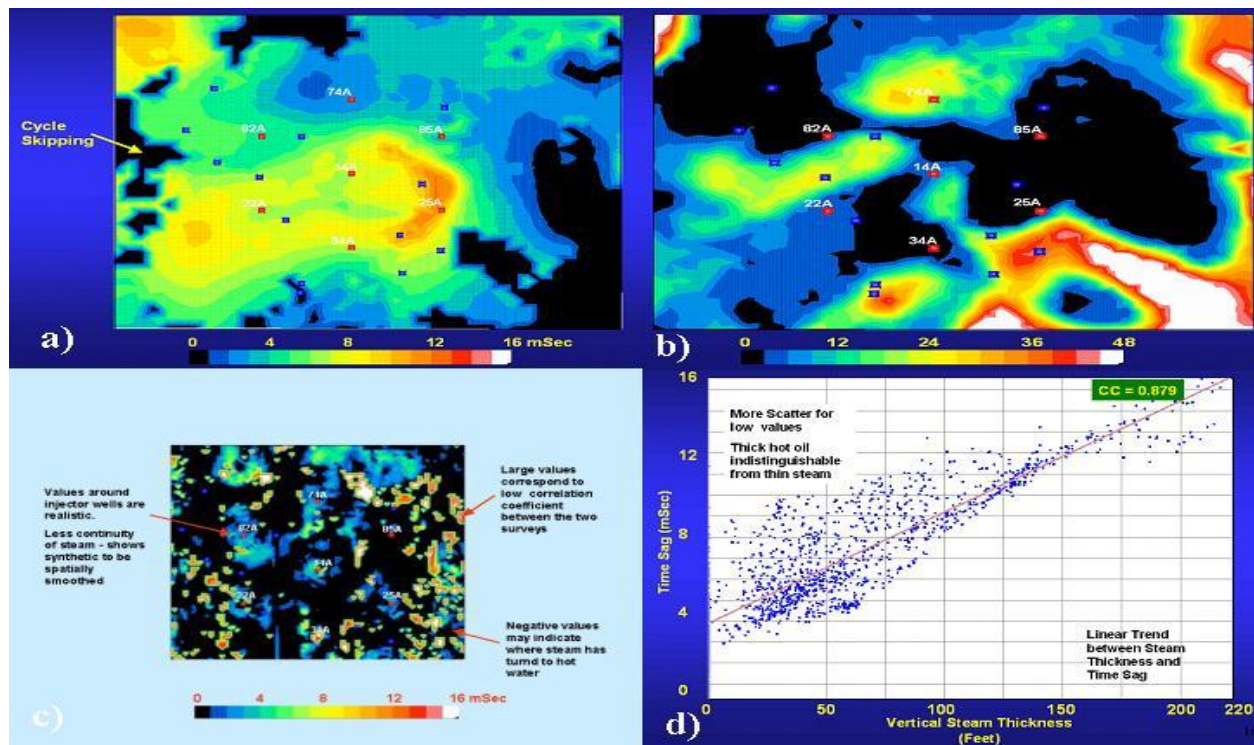
Figure 5. a).The time shift calculated at the Top Kedua using cross-correlation methods, **b)** Difference in RMS Amplitude of Pertama in the synthetic model,**c)**Time shift steam effect measured by cross-correlation *Top Kedua*,**d)** Cross plot of the calculated and the vertical steam thickness determined from the earth model (*Wydiantoro and Primadi.,1998*).